Instability dynamics in immiscible binary Bose-Einstein condensates under constant forces

Lauro Tomio

Instituto de Física Teórica, UNESP
São Paulo, Brasil

FAPESP
CNPq
Conselho Nacional de Desenvolvimento Científico e Tecnológico
unesp
IFT - UNESP
INSTITUTO DE FÍSICA TEÓRICA

16 May 2025

Instituto de Física Teórica, UNESP, São Paulo

Instability dynamics in immiscible binary Bose-Einstein condensates under constant forces

Collaborators in the present work:

Sabari Subramaniyan

[Instituto de Física Teórica-UNESP, São Paulo, Brazil]

Arnaldo Gammal

[Instituto de Física da USP (IFUSP), São Paulo, Brazil]

R. Kishor Kumar

University of Otago, Dunedin, New Zealand

Resume

By considering initially immiscible configuration of binary homogeneous Bose-Einstein condensates confined in a two-dimensional circular box, I will report results of some investigation we have done considering the emergence of Rayleigh-Taylor (RT) and Kelvin-Helmholtz (KH) instabilities.

For the binary mixture, it has been considered the rubidium isotopes ^{85}Rb and ^{87}Rb. Further, it will be also reported instabilities that occur in the binary mixture when centrally and axially phase separated states are submitted to sudden transitions from immiscible to miscible regimes by reducing the inter-species interactions.

In all these cases, it will be shown the associated kinetic energy spectra as functions of the wave number k, which roughly follow the $k^{-5/3}$ and k^{-3} scaling behaviors at specific time intervals.

Quantum turbulence in Bose-Einstein condensates

This is part of a project we are following on quantum turbulence in Bose-Einstein condensates (BEC), in which we have recently studied vortex dynamics and turbulence in perturbed binary condensates (also considering dipolar BECs.):

- A.N. da Silva, R.K. Kumar, A.S. Bradley, L.T., Vortex generation in stirred binary Bose-Einstein condensates, Phys. Rev. A 107, 033314 (2023).
- S. Sabari, R.K. Kumar, L.T., Vortex dynamics and turbulence in dipolar Bose-Einstein condensates, Phys. Rev. A 109, 023313 (2024).
- L.T., A.N. da Silva, S. Sabari, R.K. Kumar, Dynamical Vortex Production and Quantum Turbulence in Perturbed Bose-Einstein Condensates, Few-Body Systems 65, 13 (2024).

This presentation is based on the preprint arXiv:2503.13767

Outline

- Introduction
  - Classical and Quantum Turbulence
  - Vortex, superfluid and turbulence dynamics
  - Rayleigh-Taylor (RT) and Kelvin-Helmholtz (KH) instabilities
- Formalism
  - Mean-field 2D model for binary BEC
  - Kinetic energy spectrum decomposition
- Numerical simulation results
  - RT instability
  - KH instability
  - Instability from immiscible-to-miscible transition
- Conclusions

Classical and Quantum Turbulence

Turbulence and vortices

As an old classical problem in physics, Leonardo Da Vinci (1952-1519), by observing a turbulent flow, described it as consisting of many vortices with different scales.
In his view, **Turbulence** is not a simple disordered state, but having some structures with vortices.

Classical and Quantum Turbulence

Vortex, superfluid and turbulence dynamics

- *Turbulent fluids* is discussed in the Feynman Lectures on Physics [pgs. 3-9, Vol. I (1963)] as a very old problem that has not been solved till now, because in physics no one has been able to analyze it from first principles.
- The dynamics of quantum fluids are governed by quantum mechanics, rather than classical physics.
- The connection of turbulence with a superfluid via the quantized vortex lines was also first suggested by Feynman.
- Now, due to some similarities found with the corresponding classical theory, a lot of expectation exists that *Quantum Turbulence* (QT) can shed some light on the general solution of such an old classical problem.
- QT actually is the name given to the turbulent flow of a fluid at high flow rates, such as superfluids.

Classical and Quantum Turbulence

- **Quantum turbulence** is an apparently random tangle of vortex lines inside a quantum fluid, as indicated by experiments and numerical solutions.
- Some examples of quantum fluids include superfluid helium (^{4}He and Cooper pairs of ^{3}He), Bose-Einstein condensates (BECs), polariton condensates.
  It is being noticed that quantum fluids exist at temperatures below the critical temperature at which Bose-Einstein condensation takes place.
- Two main questions in the study of quantum turbulence:
  - Are vortex tangles really random, or do they contain some characteristic properties or organised structures?
  - How far one can compare quantum turbulence with classical turbulence?

Classical and Quantum Turbulence

The fluid flow becomes more turbulent at high-velocity fields or when it has a high Reynolds number, which is a well-known dimensionless quantity to measure the differences in the fluid's speed and direction. For low Reynolds numbers, the flow tends to be more laminar, delaying the transition point to a turbulent fluid [Reynolds, Philos. Trans. R. Soc. 174, 935 (1883)].

Most flows in physical systems in nature are turbulent. Turbulence in low-temperature systems, which includes superfluid and Bose-Einstein condensate (BEC), is named as quantum turbulence QT).

The first experimental observation of QT was found in ^{4}He superfluid [Vinen, Proc. R. Soc. 240, 128 (1957)]. In atomic BECs, the first reported realization we have by Henn et al. [PRL 103, 045301 (2009)]

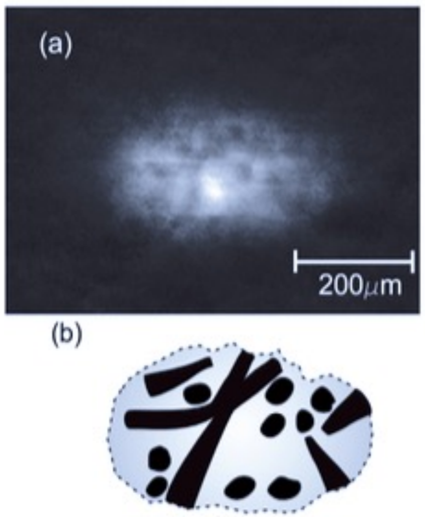

FIG. 2: (a) Atomic optical density after 15ms of free expansion showing vortex structures spread all around the cloud resembling the vortex tangle regime proposed in Ref. 8 and (b) Schematic diagram showing the inferred distribution of vortices as obtained from image shown in (a).

Kobayashi-Tsubota, PRA76 (2007) 045603

E.A.L. Henn · J.A. Seman · G. Roati · K.M.F. Magalhães · V.S. Bagnato   J Low Temp Phys (2010) 158: 435–442

Fig. 3 (Color online) **(a)** Side-by-side images of a regular, non-excited BEC and a turbulent cloud showing the aspect ratio inversion on the former case and the suppression of that inversion in the turbulent regime. **(b)** Aspect ratio (ratio between main axes) of the BEC and turbulent clouds evidencing the inversion of the first and maintenance of the latter

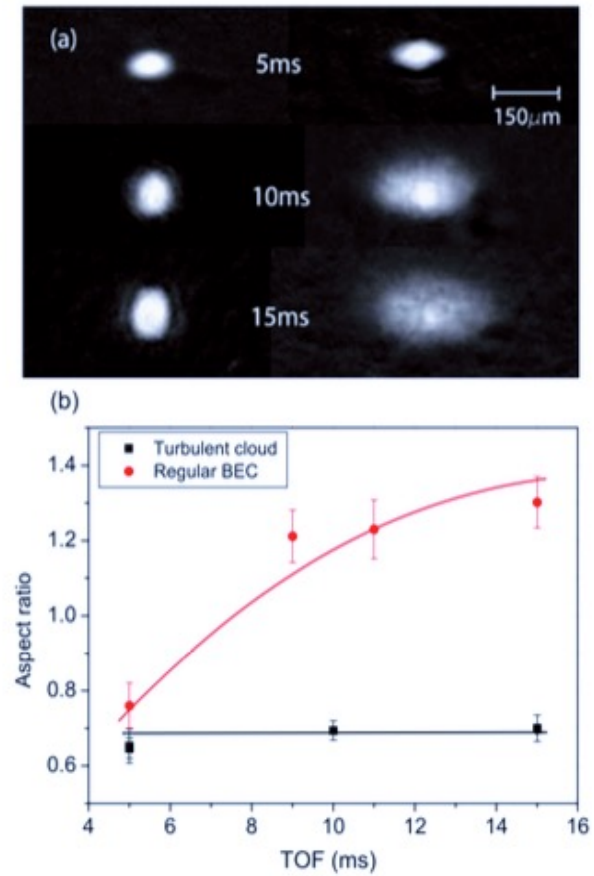

The experiments with BEC have attracted more attention concerning the properties of QT because of the actual advanced cold-atom laboratory techniques, which are more helpful in controlling the condensate parameters.

So, a few years later, other relevant experiments have been done, such as by Navon et al. Nature 539 (2016) 72.
The evolution of large clusters with ^{87}Rb BECs has been also demonstrated by
Gauthier et al., Science 364 (2019) 264;
and in Johnstone et al., Science 364 (2019) 1267, by considering 2D superfluid.
These experiments on QT have also identified the emergence of a Kolmogorov's scaling [Kolmogorov1941] in the energy spectrum, with vortex structures associated to a *k^-(5/3 power law) in* the infrared region.

The studies on turbulence and vortex patterns in multicomponent BECs are interesting due to different miscibility properties.
The binary mixtures show rich pattern varieties, that can lead to **Rayleigh-Taylor (RT)** and **Kelvin-Helmholtz (KH)** instabilities [for details and refs, see Sharp, Physica D12 (1984) 3 for a review, Takeuchi et al, PRB81 (2010) 094517, and Kobyakov et al, PRA89 (2014) 013631.]

The RT instability can be exemplified by the process started at the interface between two plane-parallel immiscible fluids, under the gravity field, with the denser fluid at the top of the less dense one. Broken the equilibrium, the fluid at the top moves downward, resulting in the formation of mushroom heads of the denser fluid inside the space first occupied by the less dense one.

The KH instability occurs when there is a velocity difference across the interface between the fluids.

Model approach in BEC

In our study, we assumed QT binary BEC mixtures confined in a quasi-2D circular box, assuming the coupled ^{85}Rb-^{87}Rb system. With components spatially separated, the homogeneous density distribution is prepared in the ground-state (gs), within immiscible conditions (inter-species a_{12} larger than the intra-species interactions $a_{11} = a_{22}$).

The RT and KH instabilities are produced by starting with the mixture in an immiscible regime. Next, we follow with the analysis of associated patterns and vortex formations.

The RT instability is induced by the help of an initial time-independent sinusoidal perturbation (in a short time interval), which is applied to the ground-state solution, followed by linear forces applied to the mixture components.
The KH instability is induced by a constant linear force perturbation, providing attraction between the initially separated species.

Next, we also consider a third approach to the binary mixture, by investigating the dynamics response to a sudden transition between immiscible to miscible system, obtained by fast reduction of the inter-species interaction a_{12}.
In this case, two possible initial separated configurations are applied.

All the above-mentioned scenarios induce plenty of vortex dipoles and turbulent flow in the condensates. In order to analyze them, we calculate the **compressible and incompressible kinetic energy spectrum**, as to understand how these instabilities are developed in the binary mixtures. Therefore, we search for kinetic energy regions, in which some possible universal scaling law could emerge, which could bring some consistency with the classical Kolmogorov's scaling.

Mean-field model for binary BEC

GP dimensionless 2D formalism

The coupled Gross-Pitaevskii (GP) equation for the binary system is cast in a dimensionless 2D format, with energy and length units given, respectively, by $\hbar\omega_\perp$ and $l_\perp \equiv \sqrt{\hbar/(m_1\omega_\perp)}$, in which the first species is being used as the reference for our length unit. Correspondingly, $\mathbf{r} \to l_\perp \mathbf{r}$ and $t \to t/\omega_\perp$.

We assume strongly pancake-shaped harmonic traps with fixed aspect ratios $\lambda = \omega_{iz}/\omega_{i\perp}$, where ω_{iz} and $\omega_{i\perp}$ are, respectively, the longitudinal and transverse trap frequencies for the species i. These frequencies are also assumed the same for both species, with $\omega_\perp = 2\pi\times$ 10Hz, and $\omega_z = 2\pi\times$ 500Hz, such that $\lambda = \lambda_i =$50. In order to have both particles trapped with the same aspect ratio, we need $m_1\omega_{1z}^2 = m_2\omega_{2z}^2$, implying $\omega_{2z} = \omega_{1z} \approx 0.99$.

2D coupled dimensionless GP equation for the components:

$$\mathrm{i}\frac{\partial\psi_i}{\partial t} \quad = \quad \left\{\frac{-m_1}{2m_i}\nabla_2^2 + V_i(x,y) + \sum_{j=1,2} g_{ij}|\psi_j|^2\right\}\psi_i$$

where ψ_i are normalized to one and the contact interactions, related to the scattering lengths a_{ij} ($a_{11} = a_{22}$), are expressed by

$$g_{ij} \equiv \sqrt{2\pi\lambda}\frac{m_1 a_{ij} N_j}{\mu_{ij} l_\perp}, \quad \mu_{ij} \equiv \frac{m_i m_j}{m_i + m_j}.$$

where λ is the shape parameter.

The 2D confining potential $V_i(x, y)$ is initially assumed identical for both species $i = 1, 2$, given by a uniform circular box with fixed radius R and height V_0:

$$\boxed{V_i(x, y) \;=\; \begin{cases} V_0, \text{ for } \sqrt{x^2 + y^2} > R, \\ 0, \;\text{ for } \sqrt{x^2 + y^2} \leq R, \end{cases}}$$

where V_0 will be considered much larger than the chemical potentials $\mu_i \hbar \omega_\perp$ (dimensionless, $V_0 \gg \mu$).

Two-component miscibility

The condition to enter the immiscible regime, $g_{12}^2 > g_{11}g_{22}$, for $a_{11} = a_{22} > 0$, defines the threshold $\boxed{\delta \equiv \frac{a_{12}}{a_{11}} > \frac{2\sqrt{m_1 m_2}}{m_1+m_2}.}$

Within a more general relation, the miscibility can be estimated by the overlap between the densities. With ψ_i normalized to one, the overlap can be expressed by [Kumar et al., J. Phys.Com.**1**(2017)] $\boxed{\eta \equiv \int |\psi_1||\psi_2|\; dxdy}$. The overlap is also commonly defined by

$$\boxed{\Lambda = \frac{\left[\int |\psi_1|^2|\psi_2|^2\; dxdy\right]^2}{\left(\int |\psi_1|^4\; dxdy\right)\left(\int |\psi_2|^4\; dxdy\right)}.}$$

For complete immiscible cases, $\Lambda = \eta = 0$; and in the opposite complete miscible case, $\Lambda = \eta = 1$.

Kinetic energy spectrum decomposition

To analyze the turbulent behavior, the corresponding decomposition of the kinetic energy spectrum is studied, following Ashton and Anderson [PRX **2** (2012) 041001], with the 2D GP energy functional decomposed as $E = K + E_V + E_I$), where

$$\boxed{E(\psi_1, \psi_2) = \int dxdy \left\{ \sum_i \left[\frac{m_1 |\nabla_2 \psi_i|^2}{2m_i} + V_i(x,y)|\psi_i|^2 \right] + \sum_{i,j} \frac{g_{ij}}{2} |\psi_j|^2 |\psi_i|^2 \right\}}.$$

In the fluid dynamics interpretation of the GP equation, we apply the Madelung transformation, such that $\psi_i \equiv \sqrt{n_i} \exp \mathrm{i}\theta_i$, where $n_i \equiv n_i(x,y;t)$ are the species densities i, with $\theta_i \equiv \theta_i(x,y;t)$ the fluid macroscopic phase. With $\mathbf{v}_i(x,y;t) = \nabla\theta_i$, and respective density-weighted velocities $\mathbf{u}_i \equiv \sqrt{n_i}\mathbf{v}_i(x,y;t)$, $K_i = \frac{m_1}{2m_i} \int dxdy\, |\mathbf{u}_i|^2$.

Compressible and Incompressible kinetic energies

The kinetic energy is further decomposed into compressible and incompressible parts. The incompressible energy is related to vorticity, with the compressible one originated from sound waves. For the decomposition of the density-weighted velocity, $\mathbf{u}_i = \mathbf{u}_{i,I} + \mathbf{u}_{i,C}$, with $\mathbf{u}_{i,I}$ satisfying $\nabla.\mathbf{u}_{i,I} = 0$, and $\mathbf{u}_{i,C}$ satisfying $\nabla \times \mathbf{u}_{i,C} = 0$. So, the kinetic energy terms are decomposed as $K_i = K_{i,I} + K_{i,C}$. Using the Fourier transform,

$$\begin{pmatrix} K_{i,I} \\ K_{i,C} \end{pmatrix} = \frac{m_1}{2m_i} \int dk_x dk_y \begin{pmatrix} |\mathcal{F}_{i,I}(k_x, k_y)|^2 \\ |\mathcal{F}_{i,C}(k_x, k_y)|^2 \end{pmatrix}$$

$$\begin{pmatrix} \mathcal{F}_{i,I}(\mathbf{k}) \\ \mathcal{F}_{i,C}(\mathbf{k}) \end{pmatrix} = \frac{1}{2\pi} \int dx dy \, e^{-ik_x x - ik_y y} \begin{pmatrix} \mathbf{u}_{i,I} \\ \mathbf{u}_{i,C} \end{pmatrix}.$$

Within this procedure, we first obtain the spectral density in $k-$space in polar coordinates, with the final total kinetic energies obtained by integrating on $k = \sqrt{k_x^2 + k_y^2}$, as follows:

$$\begin{pmatrix} K_{i,I} \\ K_{i,C} \end{pmatrix} = \int_0^\infty dk \begin{pmatrix} \mathcal{K}_{i,I}(k) \\ \mathcal{K}_{i,C}(k) \end{pmatrix}$$

$$\begin{pmatrix} \mathcal{K}_{i,I}(k) \\ \mathcal{K}_{i,C}(k) \end{pmatrix} = \frac{m_1 k}{2m_i} \int_0^{2\pi} d\phi_k \begin{pmatrix} |\mathcal{F}_{i,I}(k_x, k_y)|^2 \\ |\mathcal{F}_{i,C}(k_x, k_y)|^2 \end{pmatrix}.$$

Numerical Simulations: RT instability

Rayleigh-Taylor instability in the binary ^{85}Rb-^{87}Rb mixture

RT instability occurs at the interface between two fluids having different densities. It happens when the lighter fluid pushes the heavier one with the support of the gravitational force. To simulate the occurrence of a similar effect in ultra-cold systems, we assume an immiscible binary mixture, in which the heavier element (^{87}Rb) starts on the top of the lighter-mass one (^{85}Rb), considering a constant force acting perpendicularly to each other. Within this model, the ground state is prepared by considering an axially phase-separated mixture, with the inter-species interaction larger than the intra-species one, with $a_{12} = 105a_0$ and $a_{ii} = 100a_0$ $(\delta = 1.05)$.

To start the dynamical instability, a small sinusoidal $x-$direction perturbation, $\cos(0.5x)$, is applied to the first component for a short time interval from $t = 0$ till $t = 2$, creating the density oscillation. The simulation follows with the sinusoidal perturbation replaced by a linear perturbation $\nu_i\, y$, which provides a constant force ν_i in the $y-$direction. This linear force is introduced to simulate some gravitational force to develop the RT instability at the interface.

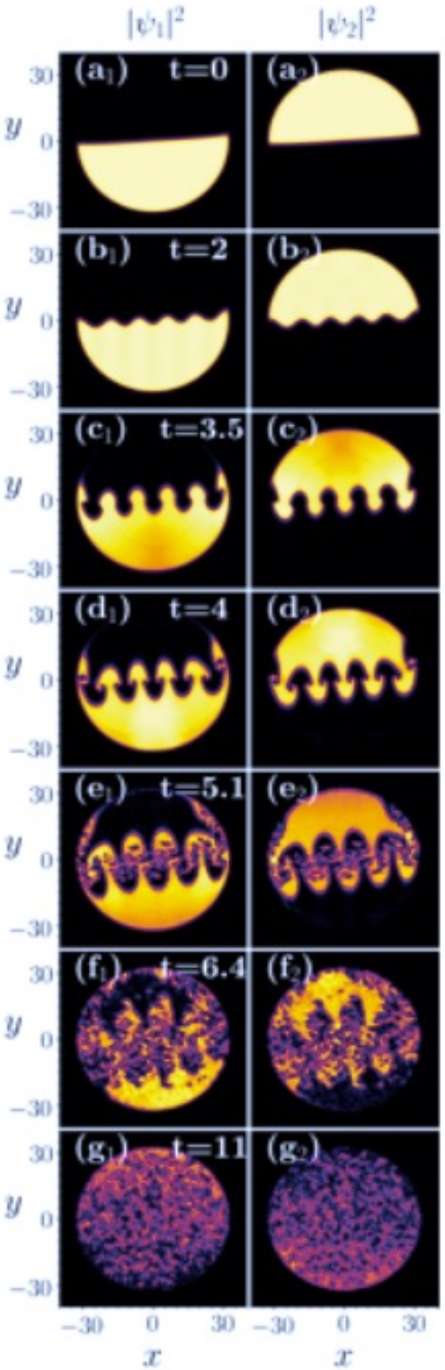

RT instability

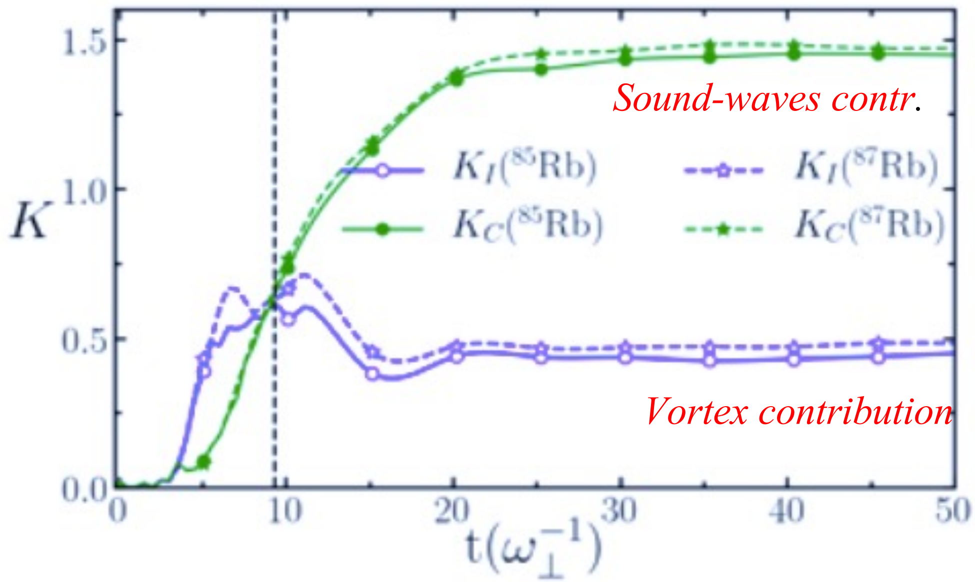

Upper: Time evolution of the incompressible and compressible kinetic energies for both components.

Left: Densities evolution of RT instability, shown by snap-shots, for the ^{85}Rb (left panels) and ^{87}Rb (right panels). The interaction ratio is kept in $a_{12}/a_{11}=1.05$ along the simulation.

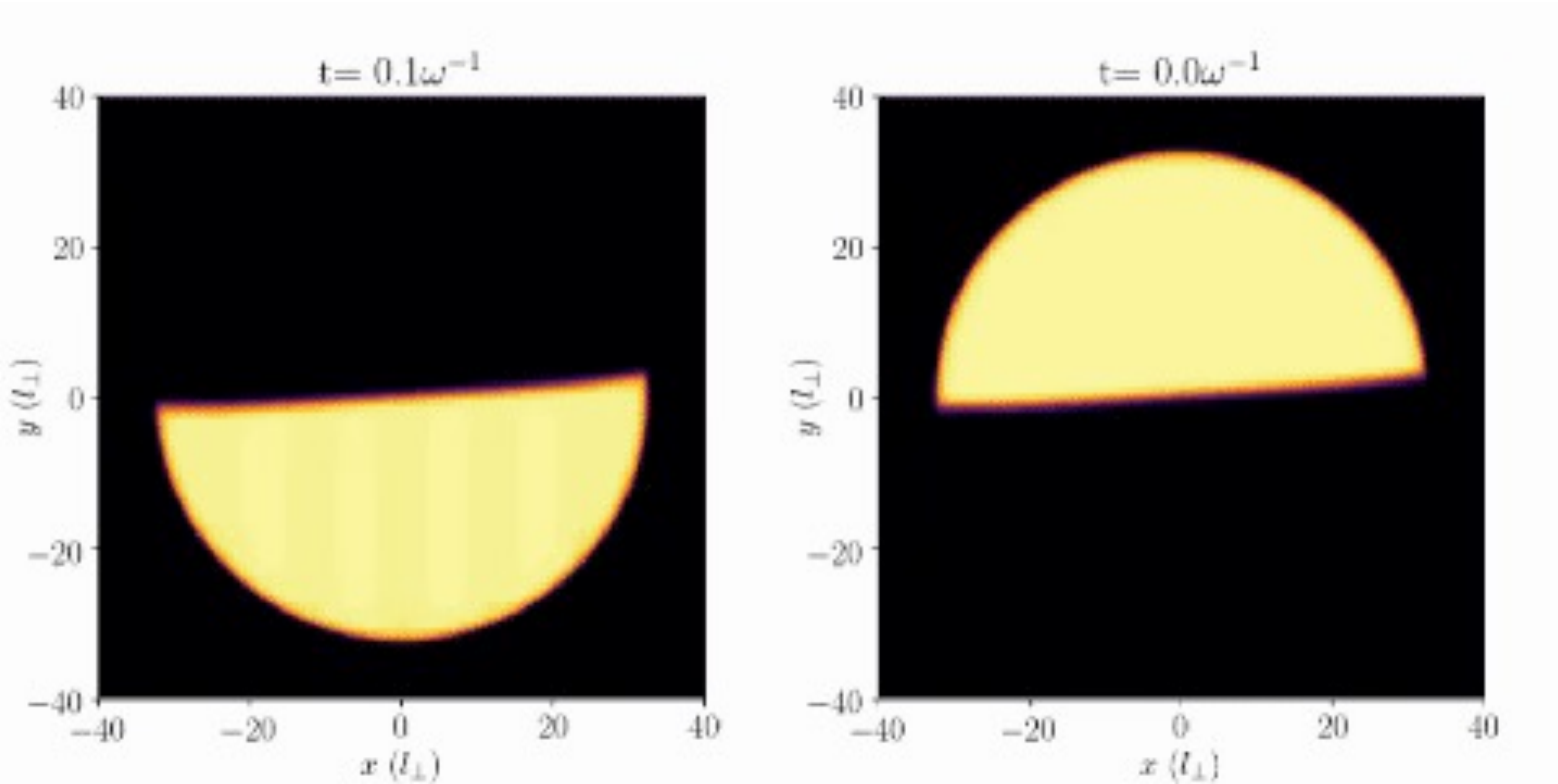

^{85}Rb ^{87}Rb

Rayleigh-Taylor Instability in binary BEC mixture

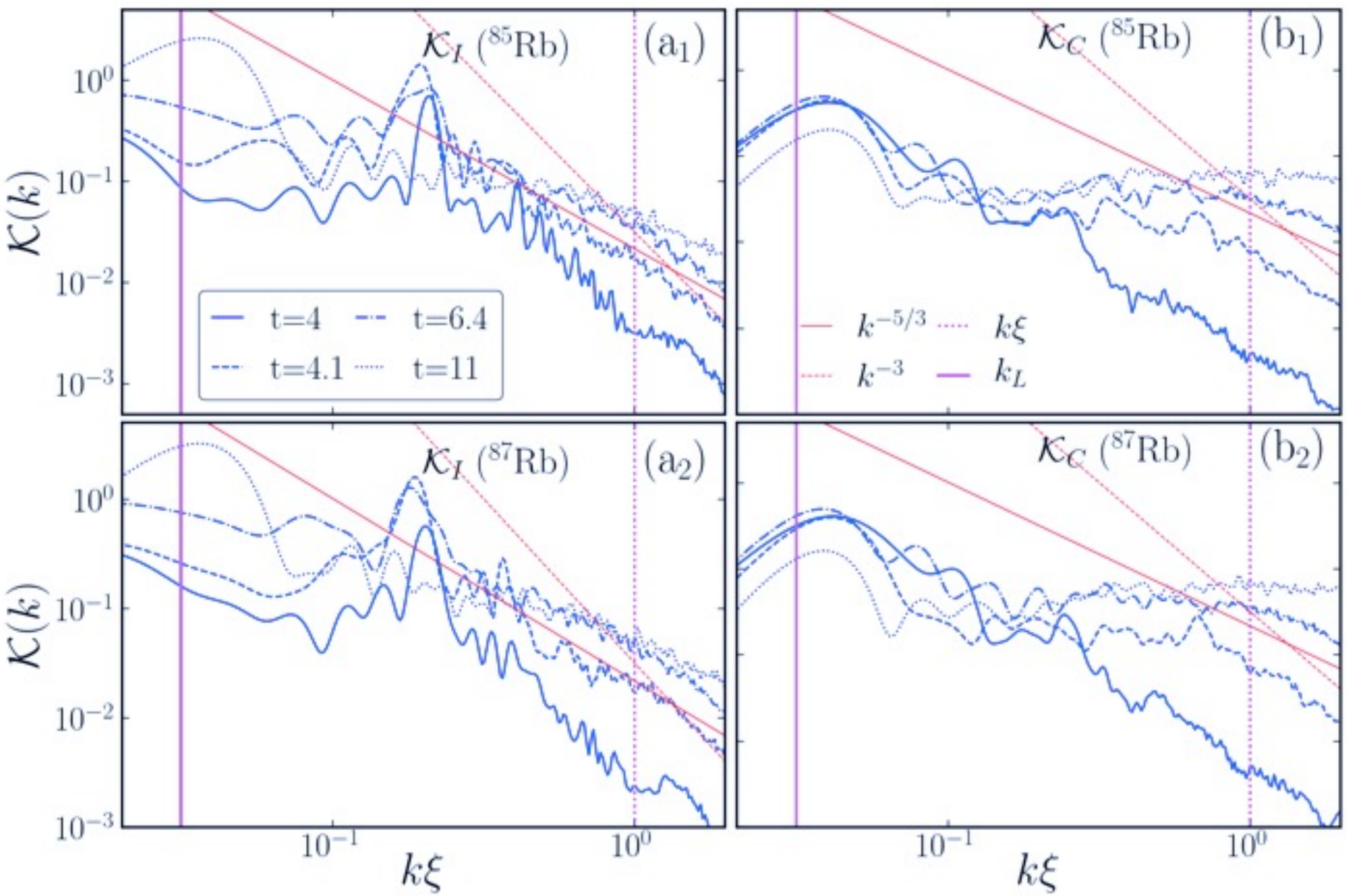

The kinetic energy spectra (incompressible and compressible), $\mathcal{K}(k)$ (units of $\hbar\omega_\perp l_\perp$), are shown for RT instability generated in the binary mixture as shown in the previous results.

Numerical Simulations: KH instability

Kelvin-Helmholtz instability in the binary ^{85}Rb-^{87}Rb mixture

KH instability occurs usually due to velocity difference across the interface in a classical fluid. It is significantly influenced by the topology of the interface. This can be simulated by introducing velocity difference between the immiscible mixtures. We consider a situation similar as the one to develop the KH instability.
For that, a linear force is applied along the x-direction, implying in a perturbation $\nu_i\, x$ in the confining potential, such that a wavy perturbation is introduced at the interface. By considering $\nu_1 = 0.7$ and $\nu_2 = -0.7$, the surface instability that can be observed is shown in the next results.

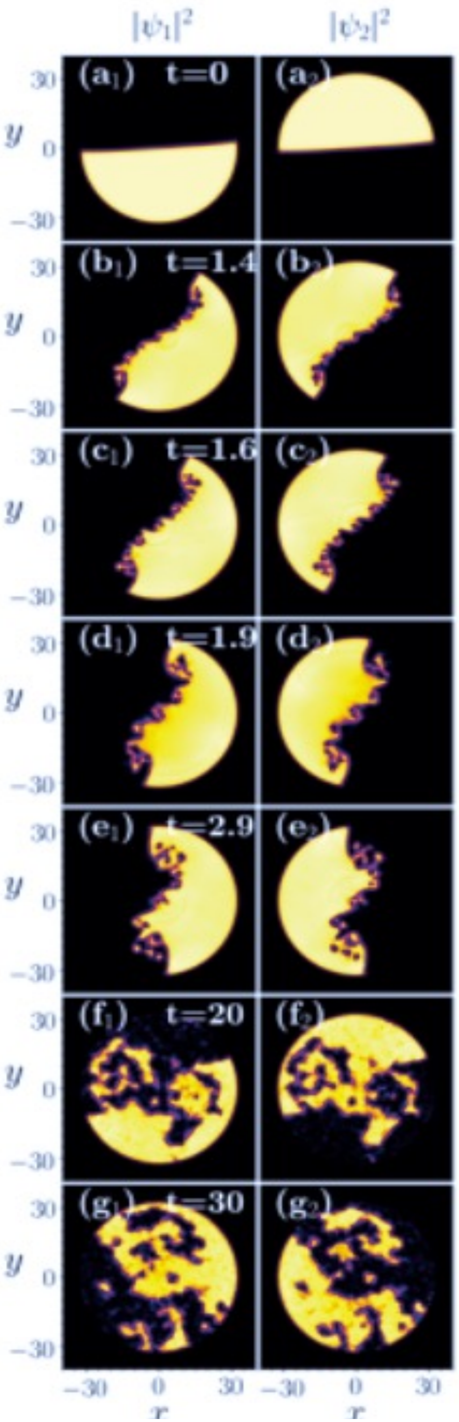

KH instability

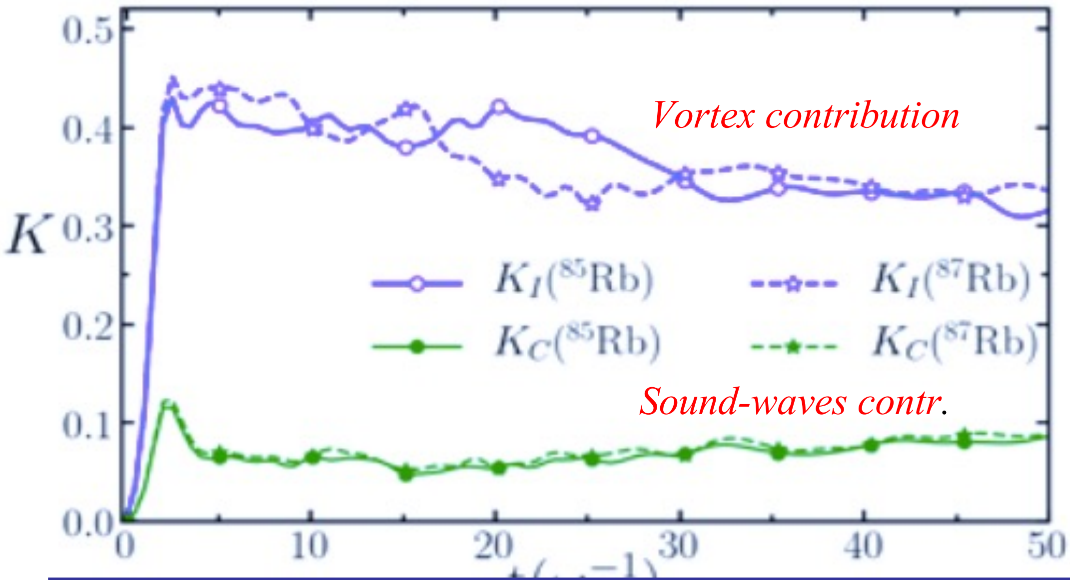

Upper: Time evolution of the incompressible and compressible kinetic energies for both components.

Left: Densities evolution of KH instability, shown by snap-shots, for the ^{85}Rb (left panels) and ^{87}Rb (right panels). The interaction ratio is kept in $a_{12}/a_{11}=1.05$ along the simulation.

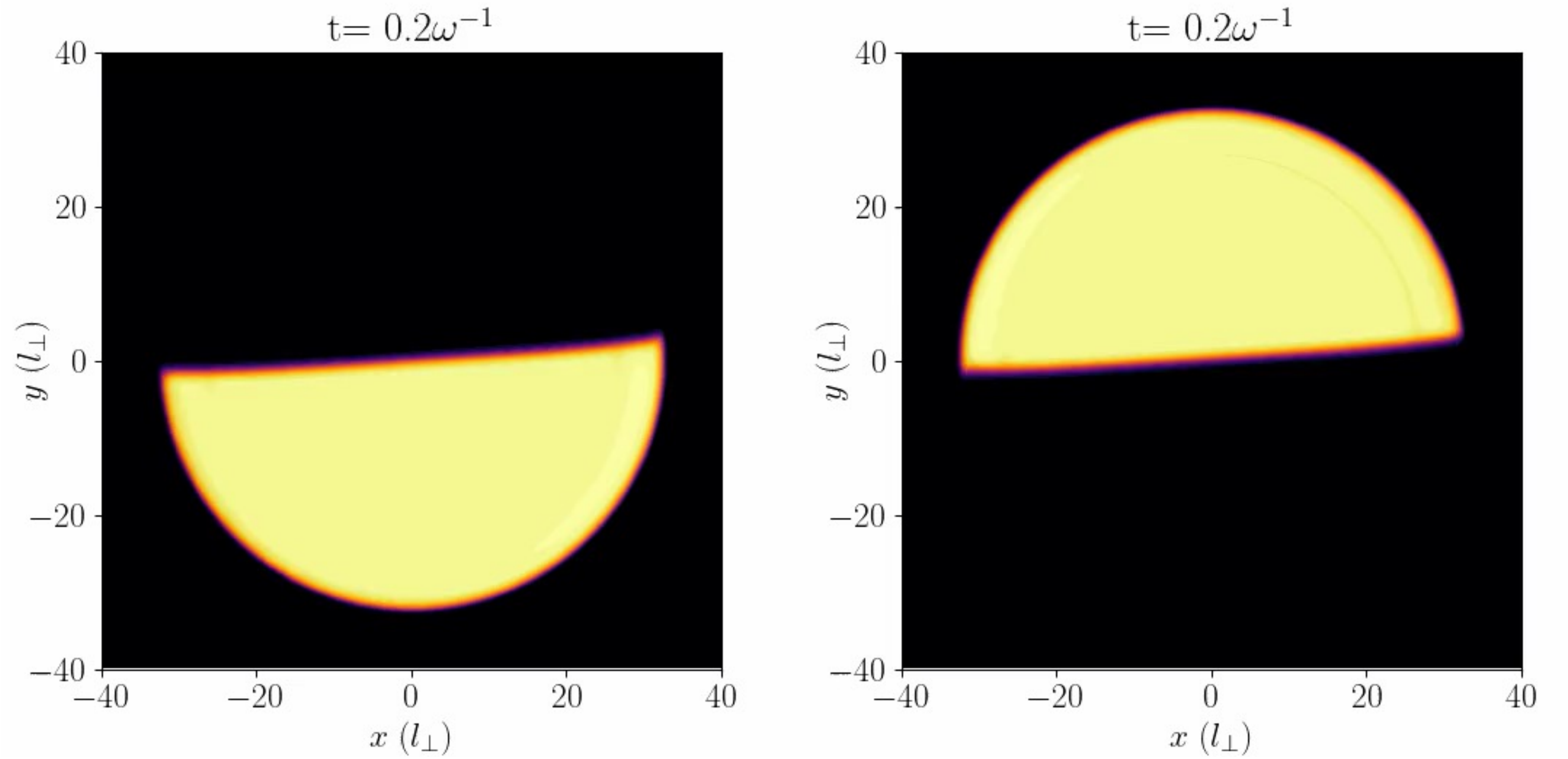
t= $0.2\omega^{-1}$
t= $0.2\omega^{-1}$
y ($l_\perp$)
x ($l_\perp$)
40
20
0
−20
−40

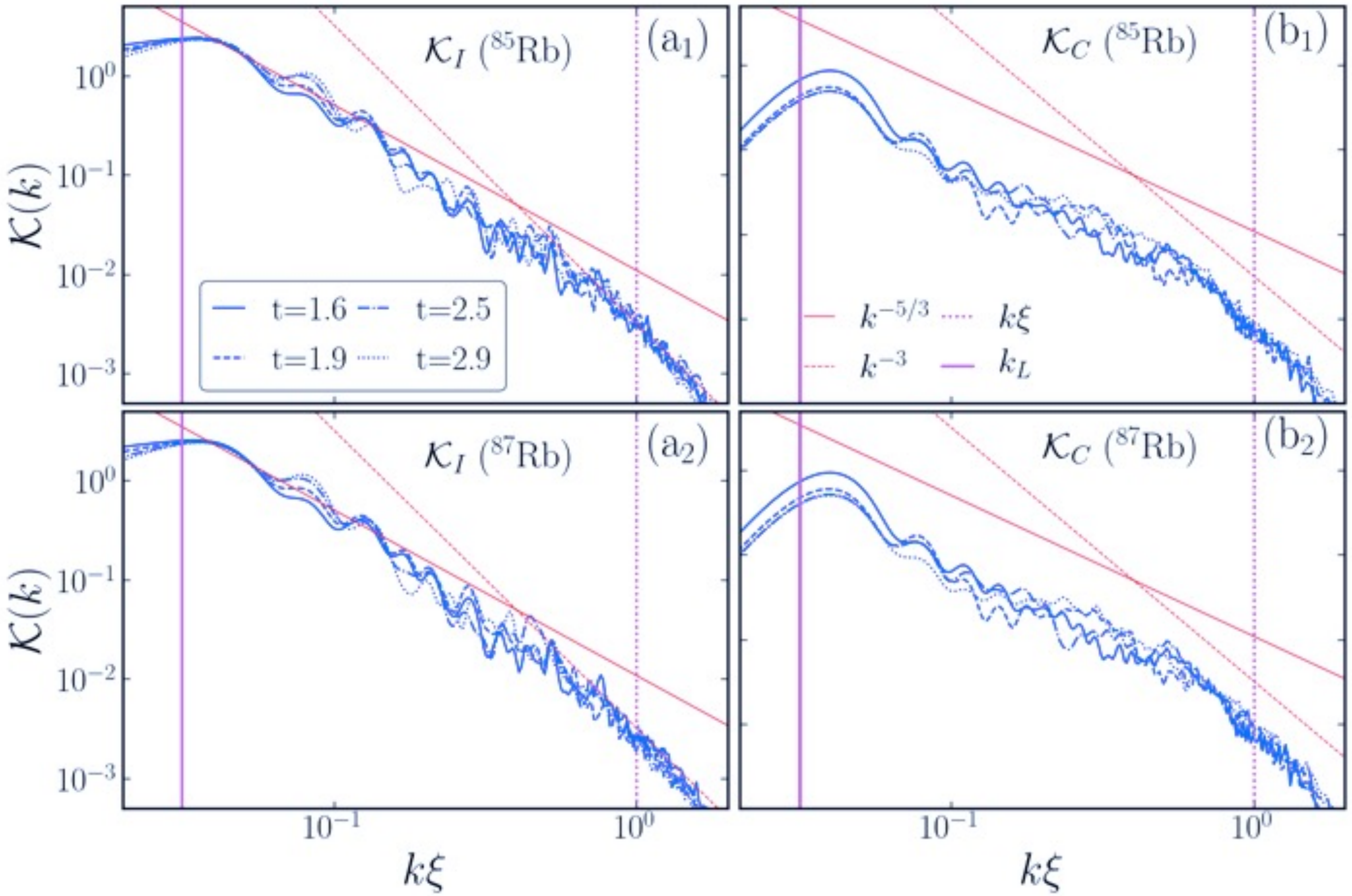

The kinetic energy spectra (incompressible and compressible), $\mathcal{K}(k)$ (units of $\hbar\omega_\perp l_\perp$), are shown for KH instability generated in the binary mixture as shown in the previous results.

Miscibility dynamics (RT and KH instabilities)

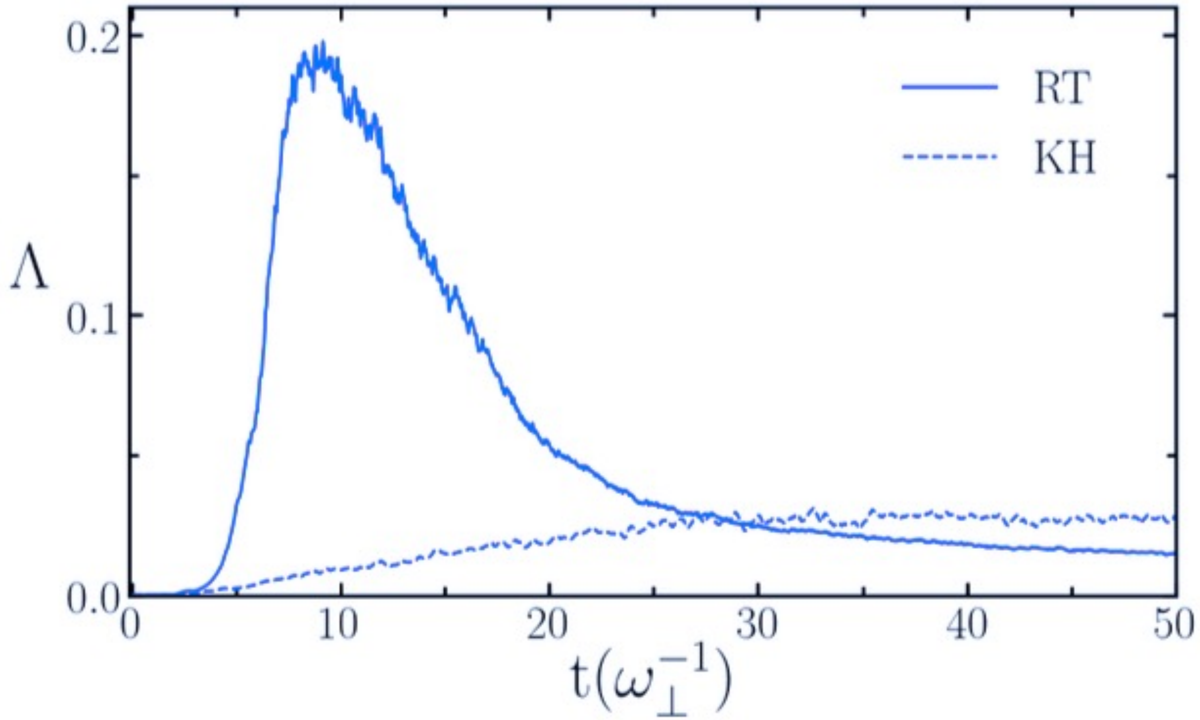

Time evolution of the density overlaps, Λ (dimensionless), for the RT (solid line) and KH (dashed line) instabilities observed in the ^{85}Rb-^{87}Rb binary mixture.

Instabilities for immiscible to miscible transition

We consider two initial configurations for the ground state of the mixture, applying a sudden reduction of the interspecies interaction, such that the system goes from immiscible to miscible.

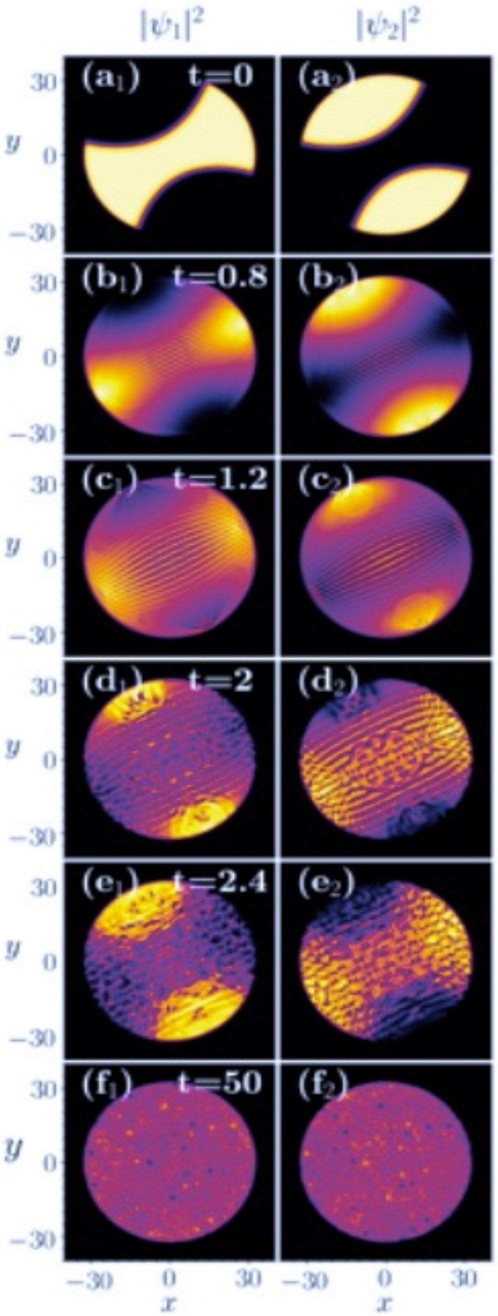

Immiscible to miscible transition
(initial centrally separated case)

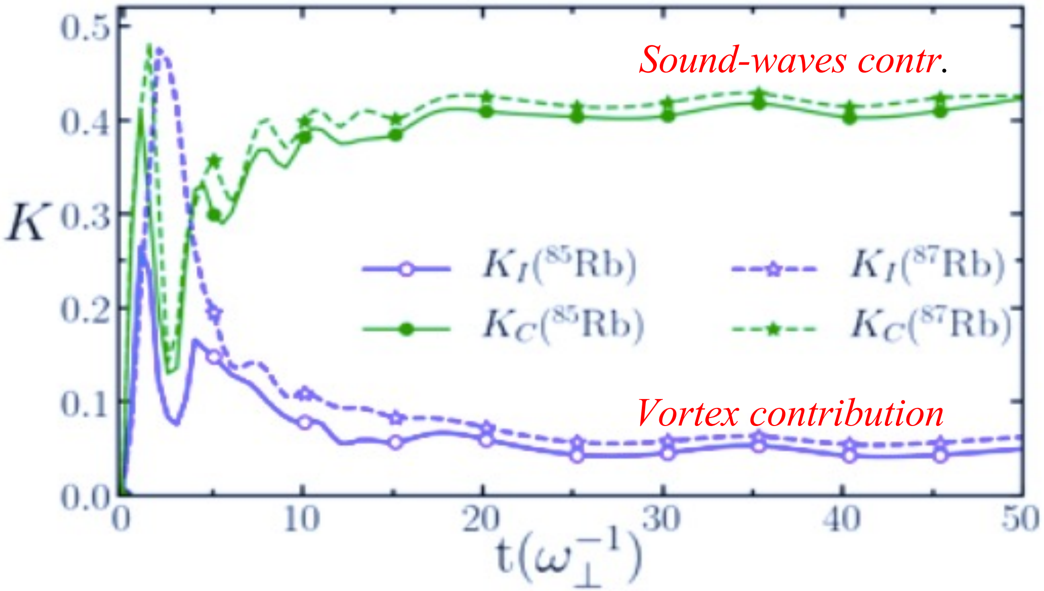

Upper: Time evolution of the incompressible and compressible kinetic energies for both components.

Left: Densities evolution in the immiscible to miscible transition for the ^{85}Rb (left panels) and ^{87}Rb (right panels) mixture, with ground-state centrally separated at t=0. The initial a_{12}/a_{11}=1.05 is changed to 0.75 in the simulation.

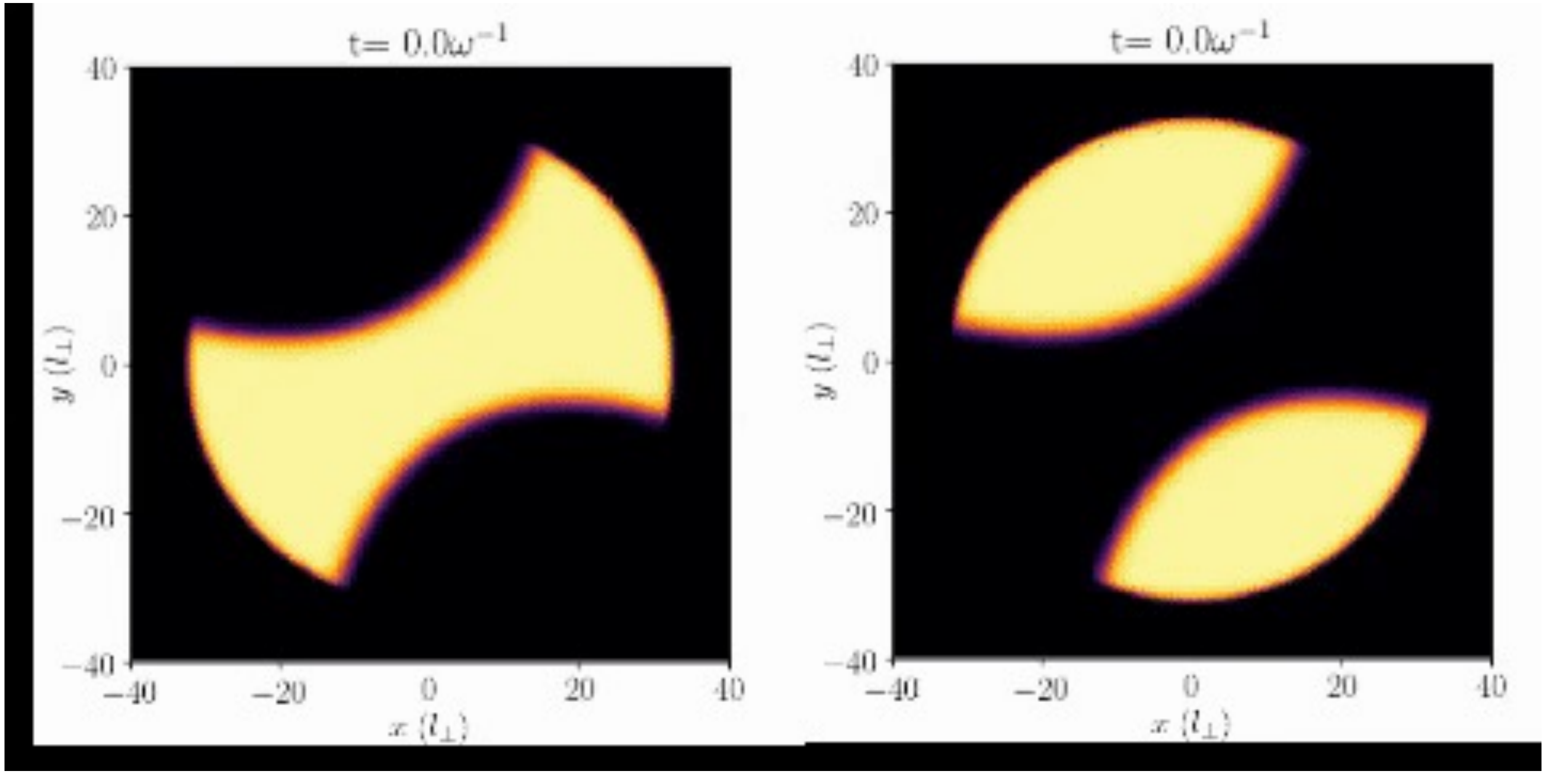

^{85}Rb ^{87}Rb

Instability in BEC mixture due to immiscible to miscible sudden transition (centrally separated initial configuration)

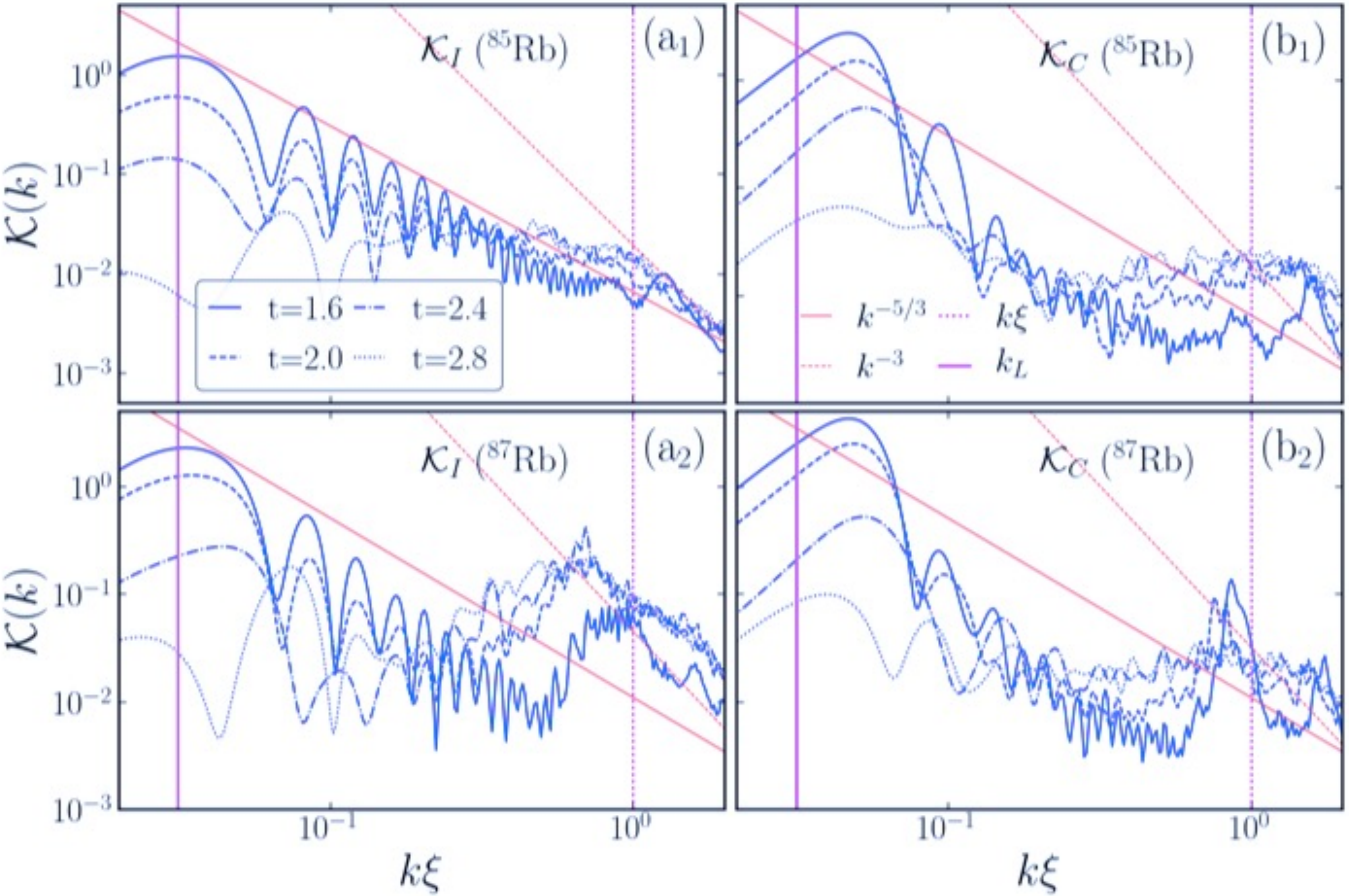

The kinetic energy spectra (incompressible and compressible), $\mathcal{K}(k)$ (units of $\hbar\omega_\perp l_\perp$), are shown for instability generated by immiscible to miscible transition considering the initial condition with centrally separated binary system.

Number of vortices in the immiscible to miscibility transition

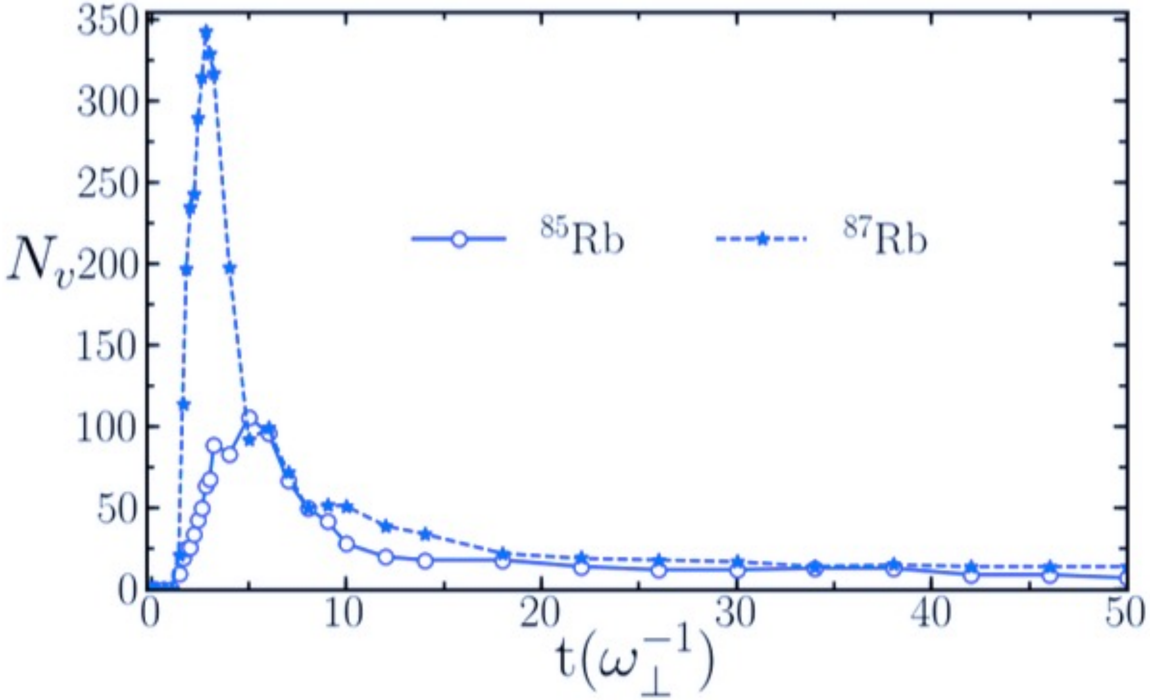

The number of vortices generated during the time evolution of both elements of the binary mixture, for the case of immiscible to miscible transition considering the initial condition with the centrally separated binary system.

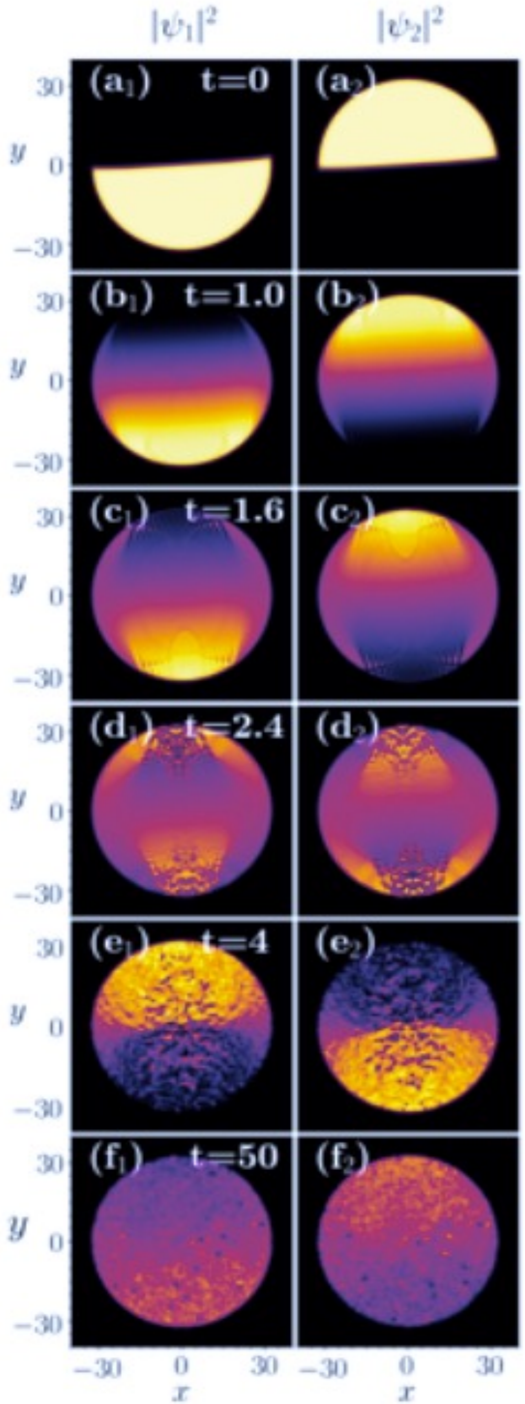

[Immiscible to miscible transition
(initial axially separated case)]()

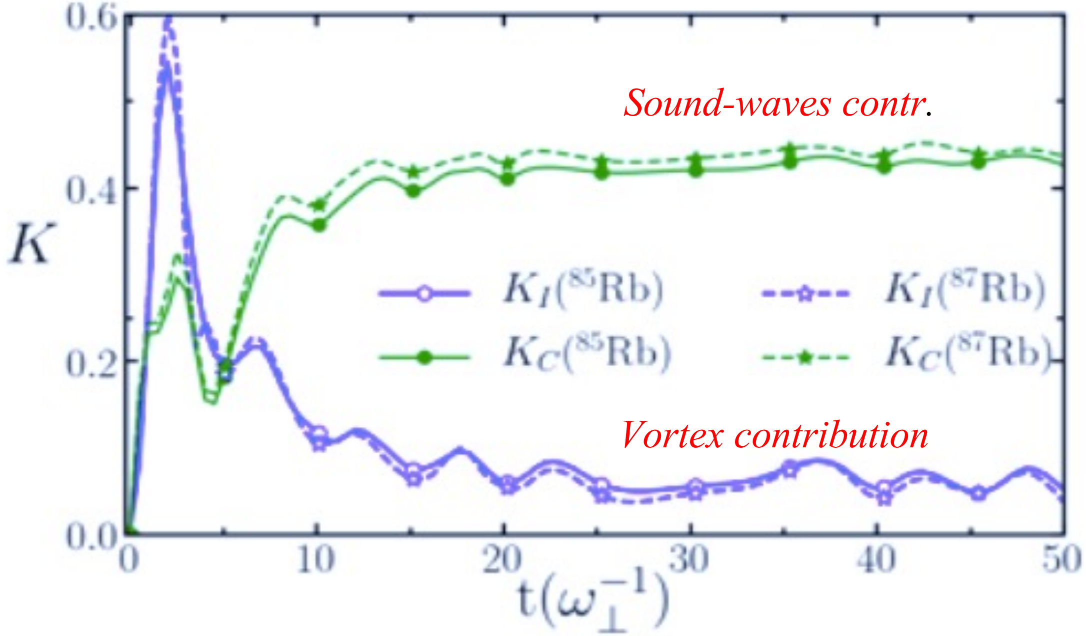

Upper: Time evolution of the incompressible and compressible kinetic energies for both components.

Left: Densities evolution in the immiscible to miscible transition for the ^{85}Rb (left panels) and ^{87}Rb (right panels) mixture, with ground-state axially separated at t=0. The initial a_{12}/a_{11}=1.05 is changed to 0.75 in the simulation.

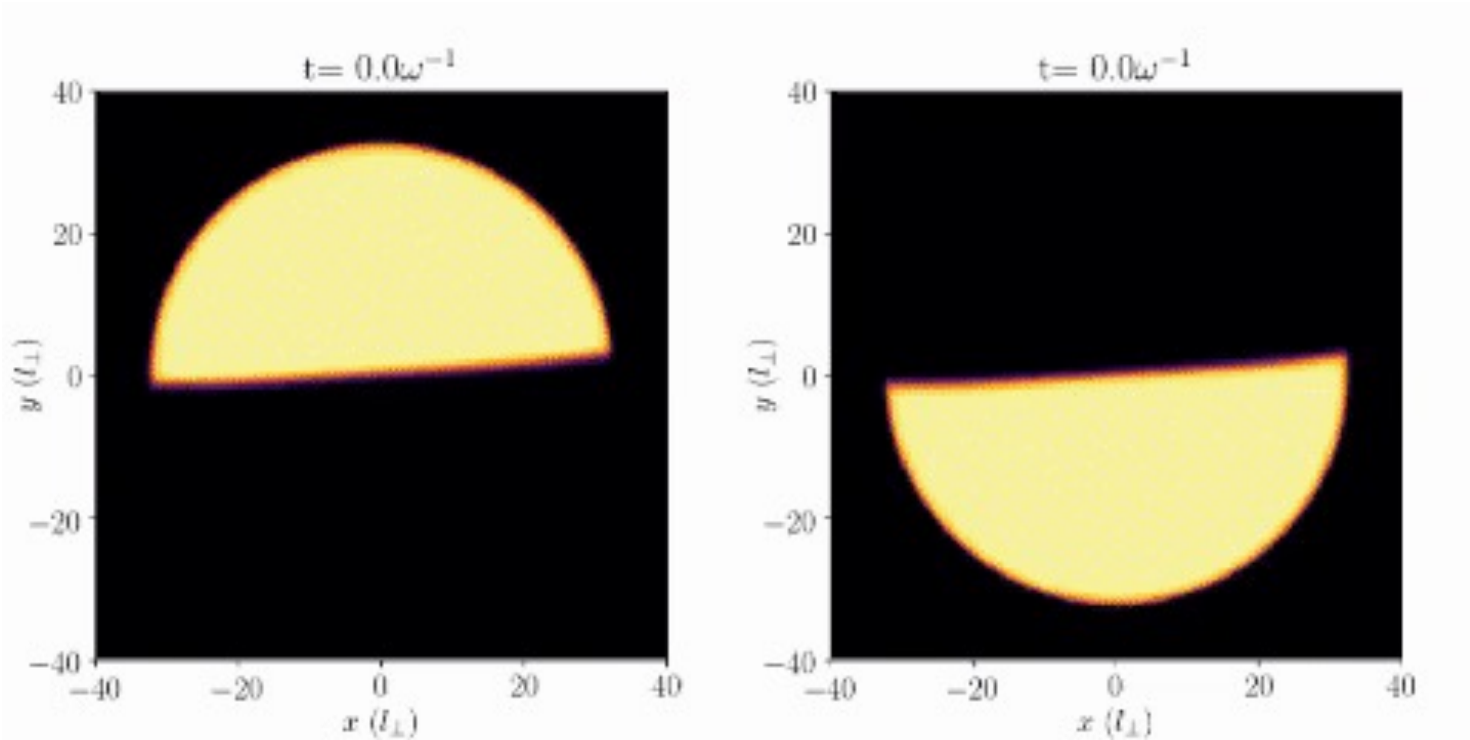

^{87}Rb ^{85}Rb

Instability in BEC mixture due to immiscible to miscible sudden transition (axially separated initial configuration)

[In this animation the lighter species is at the right]

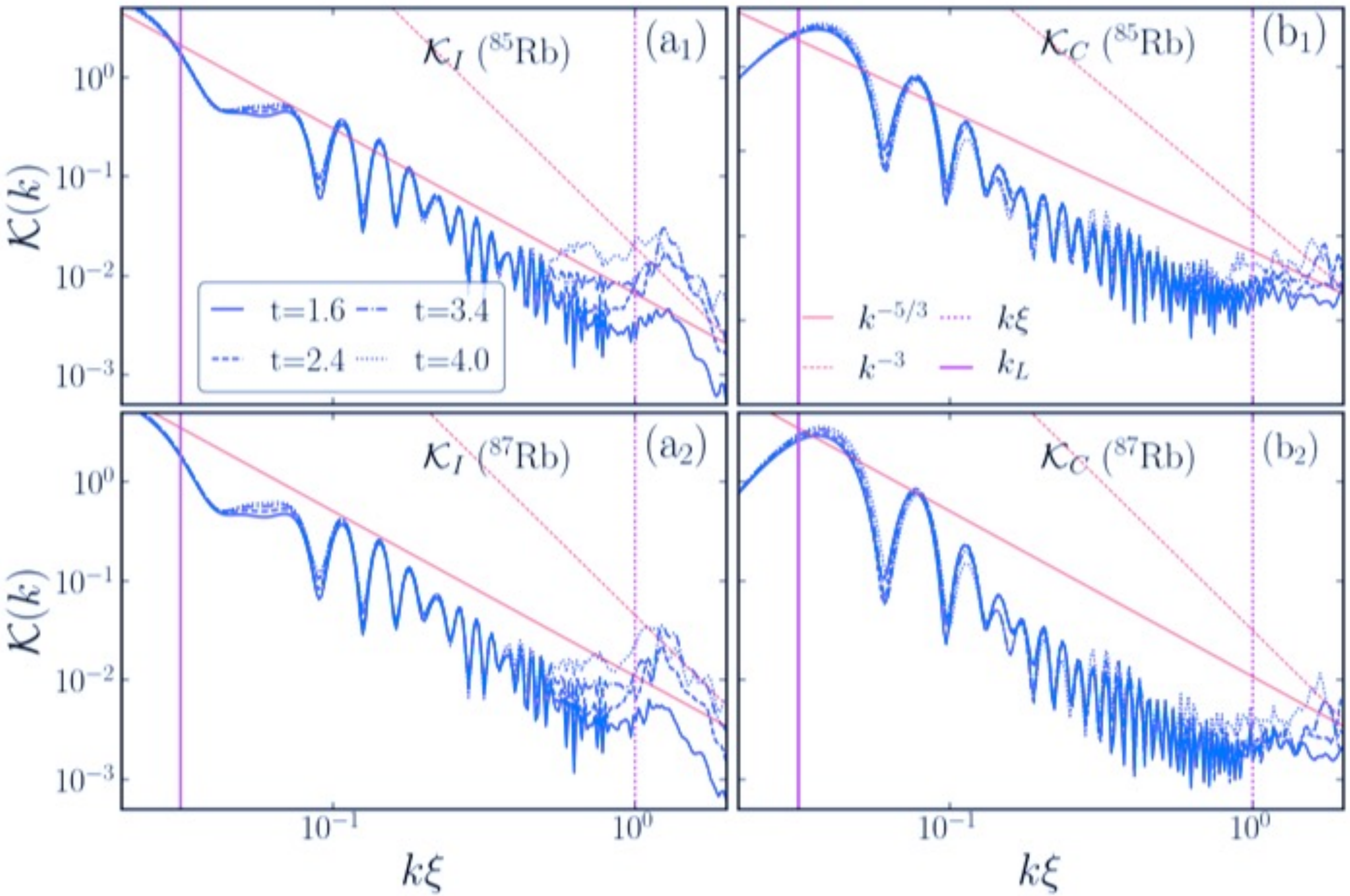

The kinetic energy spectra (incompressible and compressible), $\mathcal{K}(k)$ (units of $\hbar\omega_\perp l_\perp$), are shown for instability generated by immiscible to miscible transition considering the initial condition with the axially separated binary system.

Number of vortices in the immiscible to miscibility transition

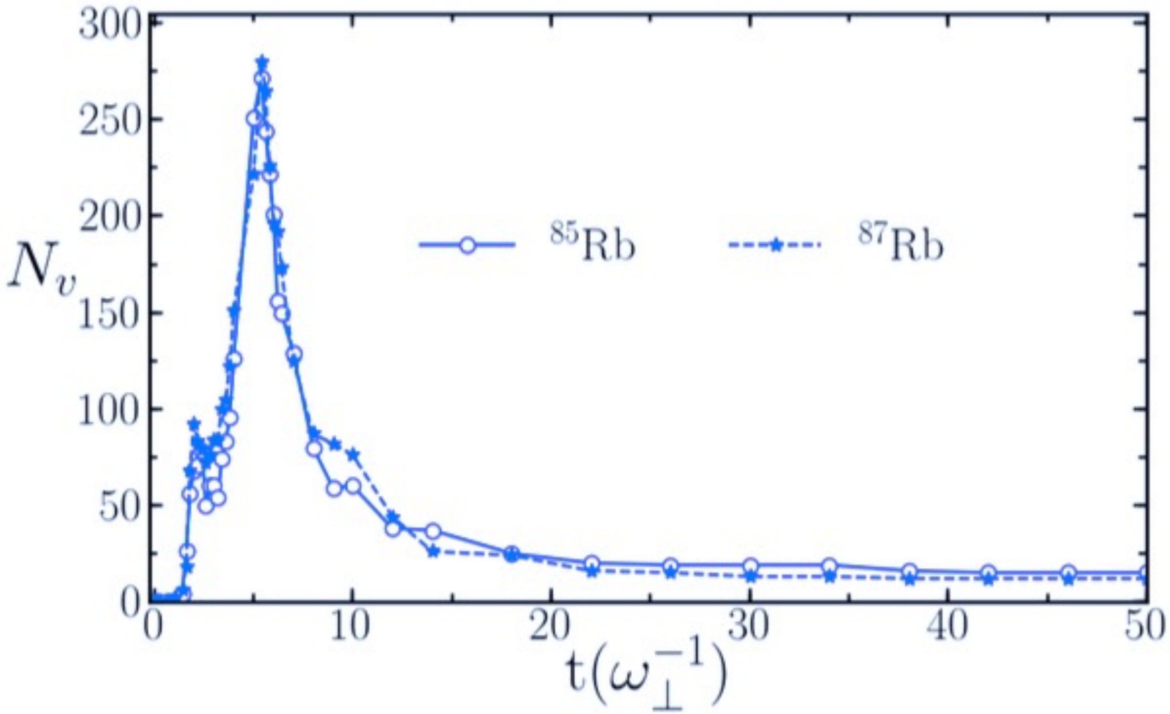

The number of vortices generated during the time evolution of both elements of the binary mixture, for the case of immiscible to miscible transition considering the initial condition with the centrally separated binary system.

Miscibility transition dependence on initial conditions

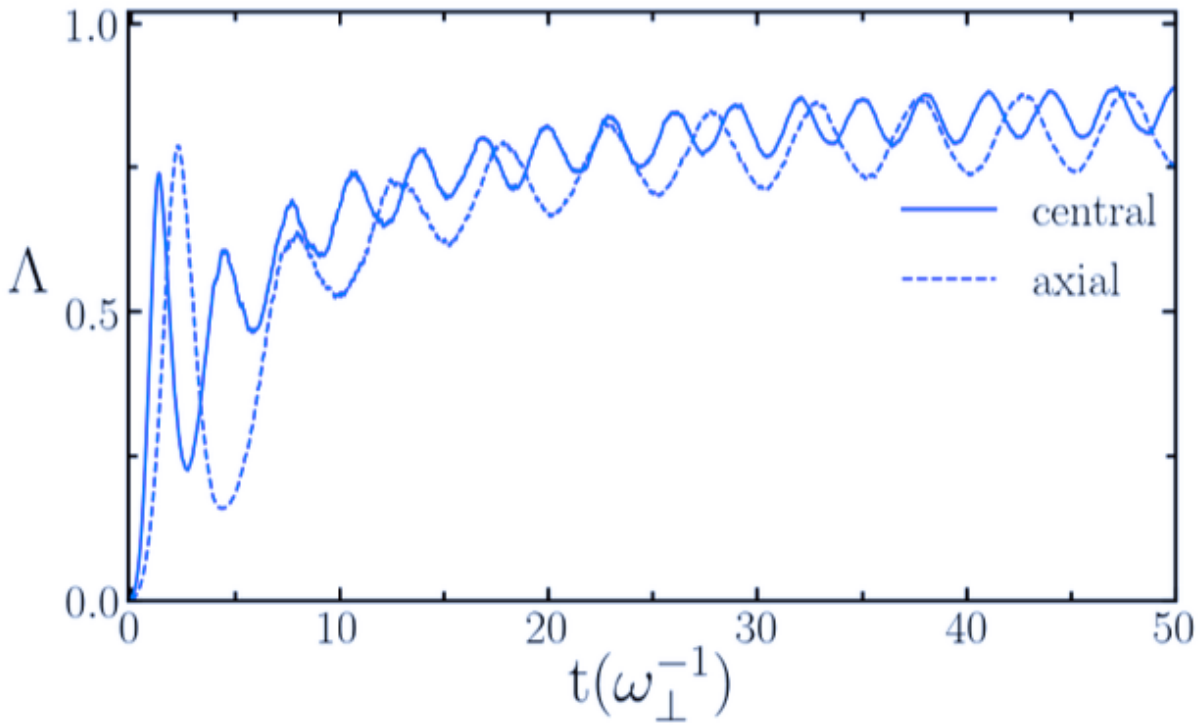

Time evolution of the density overlaps Λ, for the two initial conditions, centrally (solid line) and axially (dashed line) separated, for the binary mixture. As shown, the densities overlap from immiscible to an averaged miscible configuration.

Conclusions

Instability dynamics and QT analyses

- In our numerical simulations, using GP coupled formalism, we have studied the instability dynamics that occur in a mass-imbalanced BEC mixture, considering the rubidium isotopes ^{85}Rb and ^{87}Rb. For each case, the system was confined in a uniform 2D spherical box with a fixed radius, prepared in an immiscible configuration.
- Following spectral analyses applied to all the cases being considered for the binary mixture, the quantum turbulence behavior is studied from the time evolutions of the incompressible and compressible parts of the kinetic energy.
- The classical Kolmogorov's scaling $k^{-5/3}$ behavior can be approximately verified at short-time intervals in all the cases, considering the kinetic energy interval in which the wave number is smaller than the inverse of the healing length ($k < 1/\xi$).
- The observed vortex interactions are responsible for the appearance of sound waves, which is verified by the enhancement of the compressible kinetic energy. So, the internal energy of the turbulent condensate is increased by its kinetic energy.

Conclusions

- The time evolution of the miscibility is verified for both Rayleigh-Taylor and Kelvin-Helmholtz instabilities, which shows that no spontaneous transition occurs from immiscible to miscible systems. Only noticed is a tendency for the system to become slightly more miscible in the RT instability case, with an increase in the overlap of about 20%, but returning to immiscible configuration for larger times.
- In case of fast reduction of the inter-species interaction strength, with two different initial configurations (centrally and axially space-separation), we have verified the instability that occurs in the transition from immiscible to miscible systems.
- The number of spontaneous productions of vortices are studied. An asymmetric initial production occurs in case of centrally separated initial configuration, in which the lighter component is at the center, with less vortices being produced by the component at the center. When the components are axially separated, similar production of vortices can be verified along the evolution.

For more details, see the preprint:

Kumar, Sabari, Gammal, and LT, arXiv:2503.13767

Thank you all for the attention!

I also acknowledge partial support from the Brazilian agencies FAPESP [Projs. 2024/04174-8 and 2024/01533-7], and CNPq [Proj. 304469/2019-0].